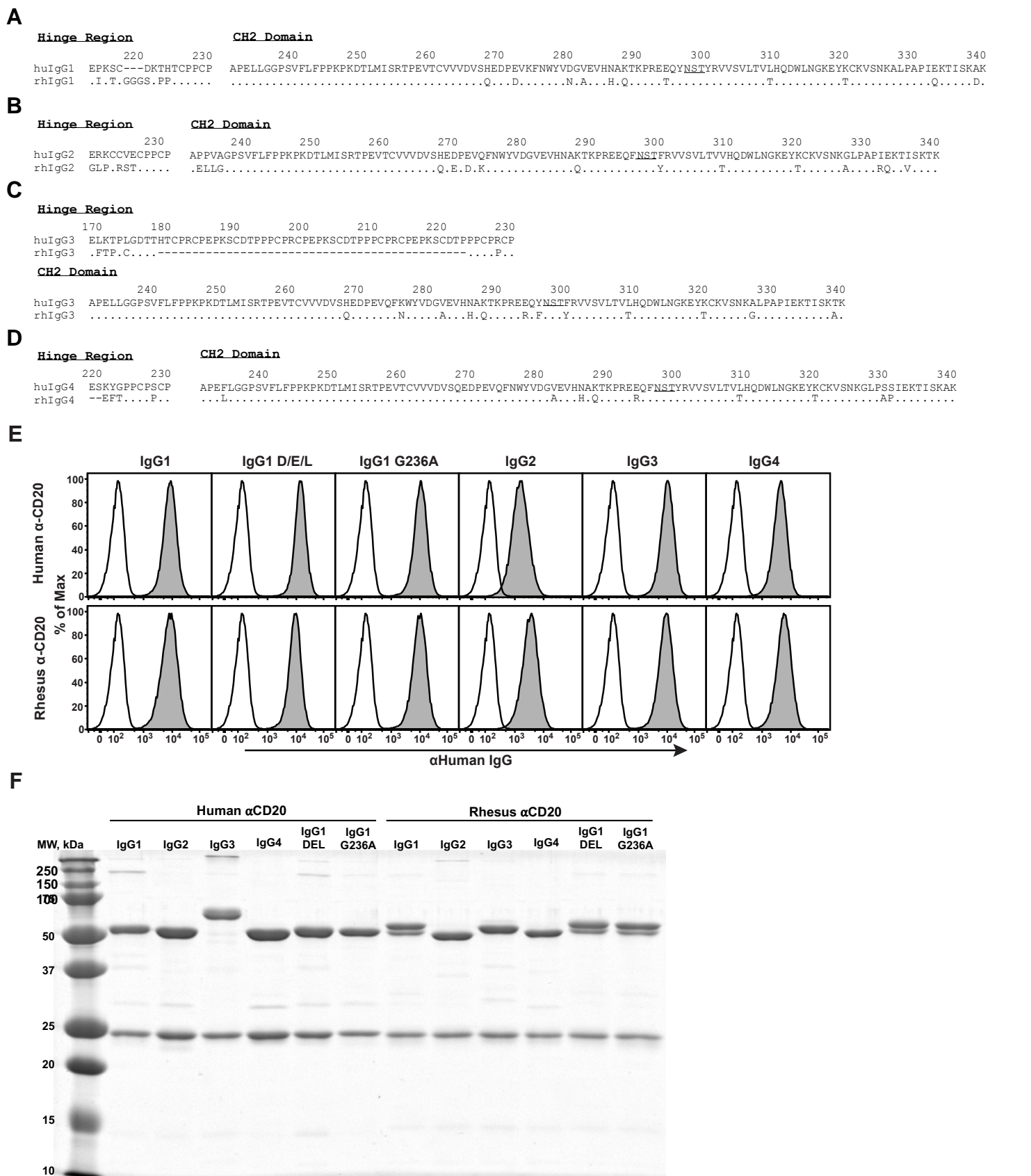
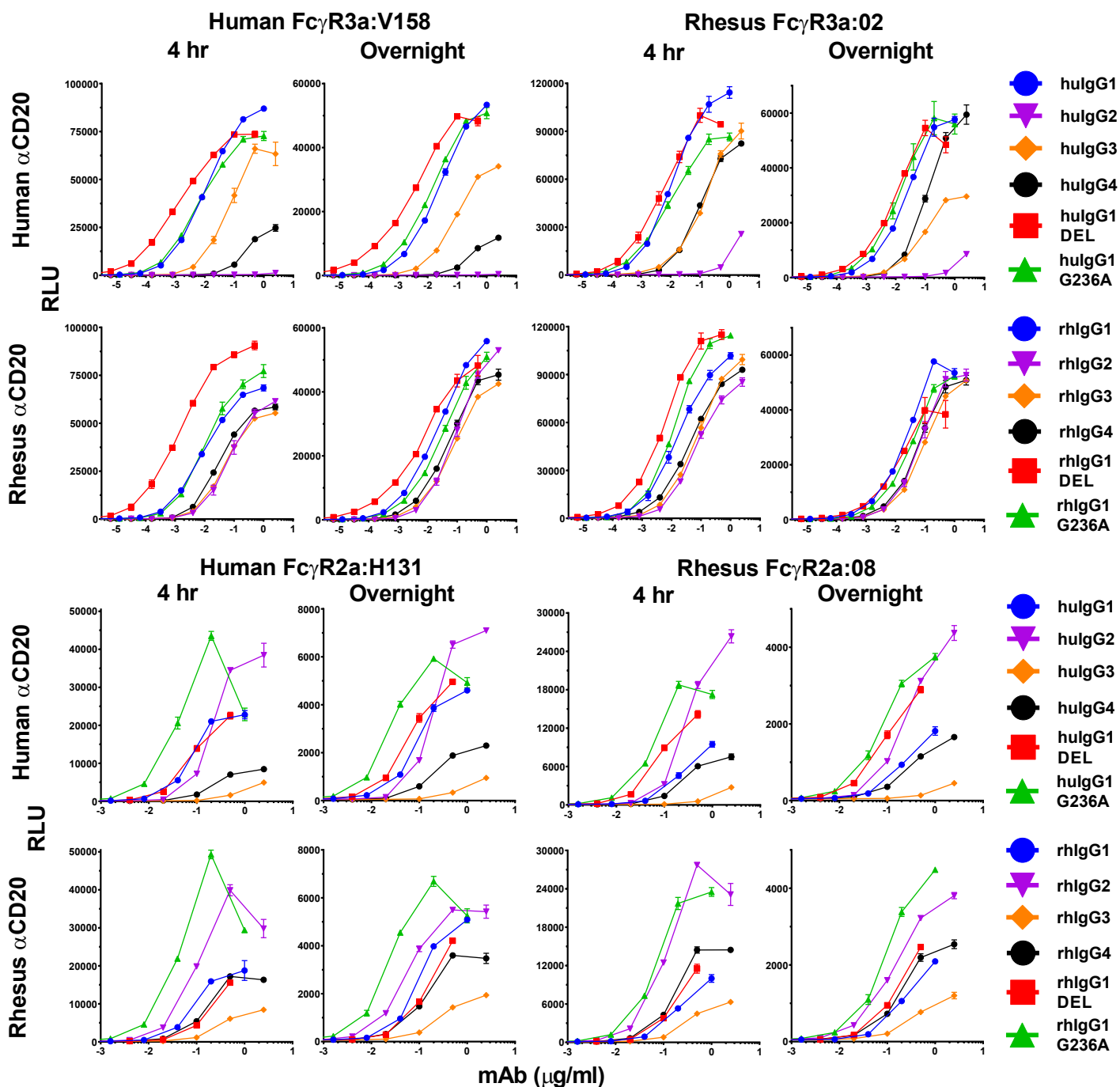


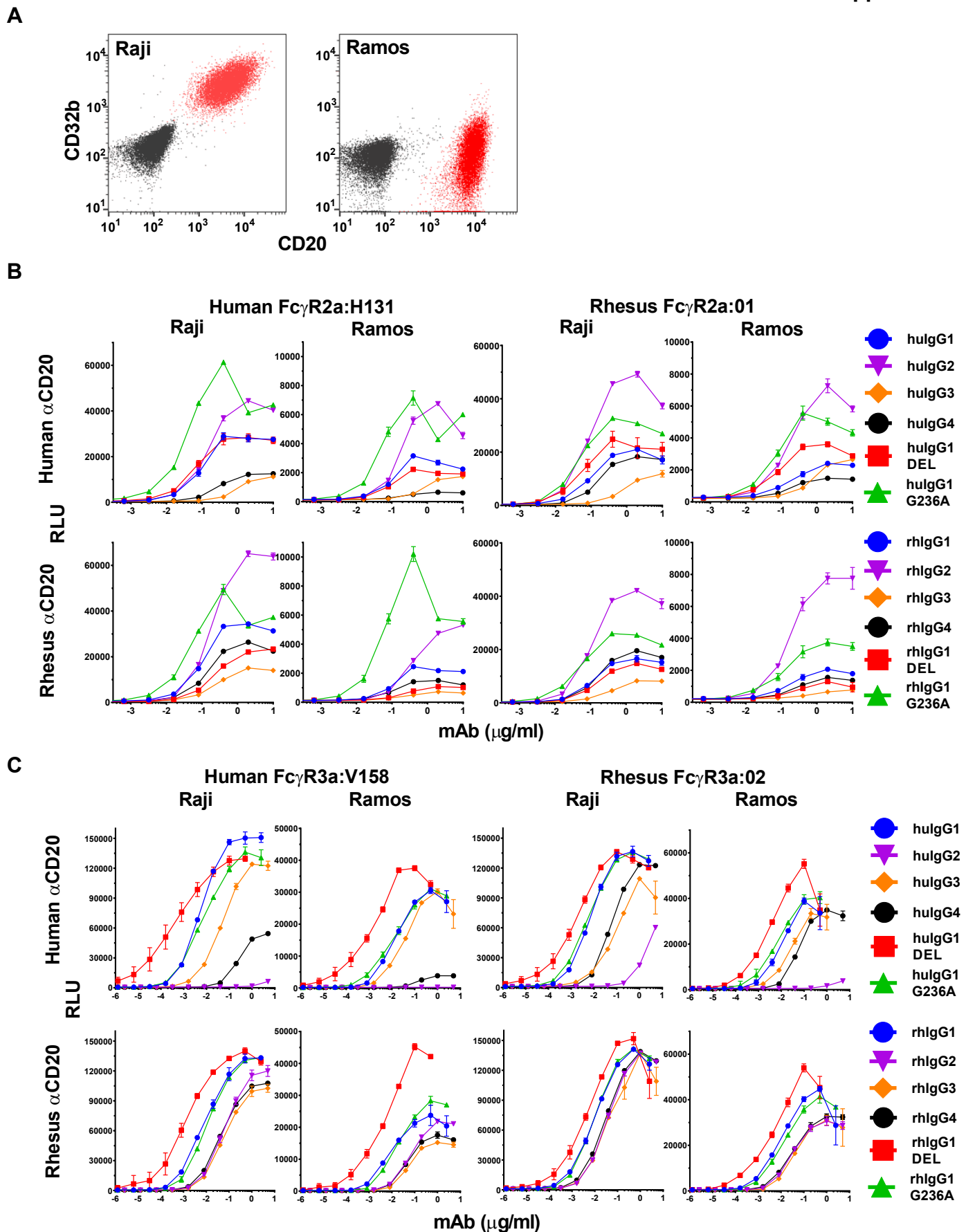
**Supplemental Figure 1.** Fc $\gamma$ R expression on the surface Fc $\gamma$ R2A- and Fc $\gamma$ R3A-transduced Jurkat NFAT-luciferase reporter cells and CD20 expression on the surface of Raji cells over time. **(A)** Human Fc $\gamma$ R2A was detected by staining with a PE-conjugated anti-CD32 monoclonal antibody (clone 2E1) and rhesus Fc $\gamma$ R2A was detected by staining with a goat anti-CD32 polyclonal antibody followed by an AF647-conjugated rabbit anti-goat antibody. **(B)** Human and rhesus Fc $\gamma$ R3A were detected by staining with anti-CD16 monoclonal antibody (clone 3G8). The histogram plots show the fluorescence intensity of staining on Fc $\gamma$ R-transduced JNL cells (shaded) relative to parental JNL cells (dotted lines). **(C)** Raji cells were stained for CD20 on three separate occasions separated by at least three weeks intervals. Cells were stained with rituximab anti-CD20 huIgG1 followed by an AF647-conjugated goat anti-human antibody. The fold-change in MFI was calculated by dividing the MFI of CD20 staining by the MFI of non-specific staining with the secondary antibody alone (mean fold-change MFI  $75.2 \pm 6.6$ ).



**Supplemental Figure 2.** Amino acid sequences of each of the four subclasses of human and rhesus macaque IgG. Alignments are shown for the hinge regions and C2 domains of human and rhesus IgG1 (A), IgG2 (B), IgG3 (C) and IgG4 (D). Positions of amino acid identity are indicated with a period, differences are identified by their single-letter amino acid code and gaps are indicated with a dash. The N-linked glycosylation site at position 297 is underlined. (E) Twelve antibodies with rituximab variable domain sequences and Fc domains corresponding to each of the human rhesus IgG subclasses, and IgG1 variants with G236A and DEL substitutions, were tested for binding to CD20. Raji cells were stained with 5 µg/ml of each antibody, followed by AF647-conjugated goat anti-human IgG secondary antibody. Dead cells were excluded by staining with Live/Dead Aqua ARC. Histogram plots show CD20 staining (shaded) compared to cells stained only with the secondary antibody (open). (F) The purity and integrity of each of the anti-CD20 antibodies was assessed by SDS-PAGE. Samples of each antibody (1 µg) were boiled in SDS sample buffer containing 5% 2-mercaptoethanol and separated by electrophoresis on a 12.5% polyacrylamide gel under reducing conditions. The heavy and light chain bands were visualized by staining with colloidal Coomassie solution and imaged using a Fujifilm ImageQuant LAS-4000 image reader.



**Supplemental Figure 3.** Comparison of 4 hour versus overnight incubation times for the JNL assay. JNL cells expressing representative alleles of human and rhesus macaque Fc $\gamma$ R2A (top panels) or Fc $\gamma$ R3A (bottom panels) were incubated with Raji cells for 4 hours or overnight with serial dilutions of rituximab anti-CD20 antibodies bearing Fc domains corresponding to different human and rhesus IgG subclasses and substitution variants. Error bars indicate SD of the mean for triplicate measurements at each antibody concentration.



**Supplemental Figure 4.** Comparison of Raji and Ramos Cell Targets in the JNL Assay. (A) Raji and Ramos cells were compared for CD20 and CD32b expression. The overlay plots show the level staining with anti-CD20 and anti-CD32b antibodies (red) relative to isotype control antibodies (black). JNL cells expressing representative alleles of human and rhesus macaque Fc $\gamma$ R2A (B) or Fc $\gamma$ R3A (C) were incubated with Raji or Ramos cells for 4 hours in the presence of serial dilutions of rituximab anti-CD20 antibodies bearing Fc domains corresponding to different human and rhesus IgG subclasses and substitution variants. Error bars indicate SD of the mean for triplicate measurements at each antibody concentration.